X-661-73-231
PREPRINT

CHARACTERISTICS OF CESIUM IODIDE FOR USE AS A PARTICLE DISCRIMINATOR FOR HIGH ENERGY COSMIC RAYS

CAROL JO CRANNELL
RICHARD J. KURZ
WALTER VIEHMANN

AUGUST 1973

GSFC

GODDARD SPACE FLIGHT CENTER
GREENBELT, MARYLAND

CHARACTERISTICS OF CESIUM IODIDE FOR USE AS A PARTICLE DISCRIMINATOR FOR HIGH ENERGY COSMIC RAYS†

Carol Jo Crannell
Federal City College
Washington, D. C. 20001

and

Richard J. Kurz
TRW Systems Group
1 Space Park
Redondo Beach, California 90278

and

Walter Viehmann
NASA/Goddard Space Flight Center
Greenbelt, Maryland 20771

Submitted to

Nuclear Instruments and Methods

†Work supported in part by NASA Grant Number NGR 09-050-001.

ABSTRACT

The possible use of CsI to discriminate between high energy cosmic ray electrons and interacting protons has been investigated. The pulse-shape properties as a function of ionization density, temperature, and spectral response are presented for thallium-activated CsI and as a function of ionization density for sodium-activated CsI. The results are based on previously published data and on corroborative measurements from the present work. Experimental results on the response of CsI to electron-induced electromagnetic cascades and to interacting hadrons are described. Bibliographies of publications dealing with the properties of CsI and with pulse-shape discrimination techniques are presented.

1. INTRODUCTION

The spectrum of high-energy cosmic-ray electrons has been measured with a variety of detectors including spark chambers, emulsions, Cerenkov radiators, scintillators, and magnetic spectrometers.[1-5] There is wide disagreement among the reported results despite persistent efforts to resolve the discrepancies. The greatest single uncertainty in determining the spectrum at energies above 5 GeV is the separation of electrons from the background of interacting protons. Those protons which interact in the first few radiation lengths of a detector can produce electromagnetic cascades which masquerade as electron-induced showers. Both analytic and instrumental techniques have been employed to distinguish between cosmic-ray electron and cosmic-ray proton primaries.

The analytic techniques, while powerful, have not been sufficiently definitive.[6] The results reported here are from an investigation of cesium iodide (CsI) for use as a totally active module in an ionization spectrometer to observe high-energy cosmic-ray electrons, protons, and heavier nuclei.

CsI is of particular interest because each signal from this material contains two types of information about the nature of the incident radiation. The intensity of the light emitted is a function of the total energy deposited; and the time dependence of the light emission, or so-called pulse shape, is a function of the ionization density or spatial rate of energy deposition. In hadronic interactions with cesium and iodine nuclei, massive low-velocity nuclear fragments are formed. The rate of energy deposition is high for these fragments and consequently high ionization densities are produced in the absorber material. Electromagnetic cascades develop rapidly because of the high atomic numbers of cesium iodine, but produce a lower ionization density for comparable total energy deposition.

An idealized approach to the development of a CsI detector which could identify interacting protons would be to determine both the properties of CsI and the pertienet properties of hadronic interactions. Then from such information the pulse shape of CsI could be predicted and optimum electronic discrimination circuitry could be designed on the basis of the anticipated response. A detector system could then be performance tested with accelerator beams of particles with known properties. While practical constraints limited the scope of the work

presented here, significant data were obtained on the properties of CsI and on its potential for use as a particle discriminator.

In the next section, the pulse-shape properties as a function of ionization density, temperature, and spectral response are presented for thallium-activated CsI and as a function of ionization density for sodium-activated CsI. The results are based on previously published data and on corroborative measurements from the present work. In the third section the response of CsI to electron-induced electromagnetic cascades and interacting hadrons is described. Bibliographies of publications dealing with the properties of CsI and with pulse-shape discrimination techniques are presented in Appendices A and B, respectively.

2. PULSE SHAPE PROPERTIES OF CsI

The time dependence of the scintillation light output of activated CsI can be well represented by a sum of exponential terms,

$$L(t) = \sum_i A_i e^{t/\tau_i}. \qquad (1)$$

The number of terms required to represent the light output adequately, as well as the parameters describing each term (A_i,τ_i), are functions of the type and concentration of the activator, the ionization density in the CsI, the CsI temperature, and the wavelength of the scintillation light. A large number of investigations of these various dependences have been performed for thallium-activated CsI. A much more limited amount of information is available concerning sodium-activated CsI. A bibliography of the available literature on the properties of CsI is given in Appendix A.

The work presented here is concerned primarily with the ionization density dependence for standard (approximately 0.1% molar) concentrations of thallium and sodium activator. For these cases two exponential terms adequately represent the scintillation light output.

2.1. Thallium-Activated CsI

2.1.1. Ionization-Density Dependence

For CsI(Tl), the basic data were obtained by Storey, Jack, and Ward (SJW).[7] SJW established that A_1, τ_1, and A_2 all depend on the ionization density produced by the exciting radiation, whereas τ_2 is independent of the ionization density. Their data are reproduced in table 1. The following definitions apply:

a. $\bar{\rho}$ is the average ionization density; defined as energy loss/pathlength in MeV/g/cm^2. For stopping particles this corresponds to kinetic energy/range. Values in the upper row in table 1 are those given by SJW. Values in the lower row are obtained from current range-energy tables.[8]

b. ε_t is the integrated light output per unit energy up to time t, i.e.

$$\varepsilon_t \equiv \int_0^t dt\ L(t)/E.$$

SJW give this quantity relative to the value of ε_t for 0.662-MeV photons. Rewriting eq. (1) in terms of light per unit energy and indicating the dependence on $\bar{\rho}$ explicitly:

$$L(t)/E = a_1(\bar{\rho})\ e^{-t/\tau_1(\bar{\rho})} + a_2(\bar{\rho})\ e^{-t/\tau_2}, \qquad (2)$$

where $a_1 = A_1/E$ and $a_2 = A_2/E$. Using eq. (2).

$$\varepsilon_t = a_1\tau_1 [1 - e^{-t/\tau 1}] + a_2\tau_2 [1 - e^{-t/\tau 2}].$$

c. R_2 is the fraction of the total light which is in the second component. Again using eq. (2),

$$R_2 = a_2\tau_2/(a_1\tau_1 + a_2\tau_2).$$

TABLE 1

Exciting Radiation	0.662-MeV photons	8.6-MeV protons	2.2-MeV protons	4.8-MeV alphas
$\bar{\rho}$	1.1	42.5	100	680
(MeV/g/cm^2)	1.5	38	82	414
τ_1(μsec)	0.70±0.025	0.60±0.02	0.52±0.01	0.425±0.01
τ_2(μsec)	7.0±0.5	7.0±0.5	7.0±0.5	7.0±0.5
ε_∞	1.0	1.18±0.05	1.04±0.05	0.48±0.03
$\varepsilon_{0.5}/\varepsilon_{4.0}$	0.385	0.476	0.476	0.588
$\varepsilon_{1.5}$	1.0	1.56±0.8	1.49±.08	0.75±0.04
R_2	0.50	0.35	0.30	0.25

No significant discrepancies with the SJW data have ever been reported by the many investigators who have measured the same properties. Measurements from this work with cosmic-ray muons and 5.3-MeV alpha particles are shown in fig. 1. While there were not sufficient data to determine the long time constant with reasonable accuracy, the short time constants were determined from these composite pulses after subtracting out the best estimate of the contribution due to the long

component. The values obtained for τ_1 are 0.78±0.08 μsec for muons and 0.53±0.06 μsec for alpha particles. The uncertainties represent scatter in the experimental points and do not include systematic effects from the measurement technique. In fig. 2, integral pulses for 4.8-MeV alpha particles and cosmic-ray muons are shown as curves from the present work together with the corresponding $\varepsilon_{0.5}/\varepsilon_{4.0}$ data from SJW. The observed consistency is quite satisfactory.

Given the normalization $\varepsilon_\infty = 1.0$ for 0.662-MeV photons, the data from SJW are sufficient to overdetermine the parameters in eq. (2) for each of the four types of exciting radiation: that is, at four values of $\bar{\rho}$. Using the definitions above, the measured values of τ_1 and τ_2 along with each measured value of ε_∞, $\varepsilon_{0.5}/\varepsilon_{4.0}$, or R_2 yields a linear relationship between a_1 and a_2 for each value of $\bar{\rho}$. In fig. 3-a, -b, -c, and -d the three relationships for each of the four values of $\bar{\rho}$ are plotted.

Once values of a_1 and a_2 are determined for the case of 0.662-MeV photons, an absolute value of $\varepsilon_{1.5}$ can be calculated for that case to determine the absolute normalization for the other three cases. Then $\varepsilon_{1.5}$ yields a linear relationship between a_1 and a_2 for each $\bar{\rho}$, which can be used to further examine the consistency of the data. This has been done in fig. 3-b, -c, and -d, where one set of lines corresponds to the ε_∞ and $\varepsilon_{0.5}/\varepsilon_{4.0}$ solution in fig. 3-a, and the other set corresponds to the ε_∞ and R_2 solution.

If eq. (1) adequately represents the actual light output and the data were internally consistent, there would be a single common inter-

section of the relationships between a_1 and a_2 in each case. Note, however, that there is a lack of agreement in each case. It is assumed here that the magnitude of the discrepancy between the various solutions indicates the accuracy of the values of a_1 and a_2 so derived. The values of a_1 and a_2, obtained from both solutions described above, are plotted as functions of $\bar{\rho}$ in fig. 4. It can be seen that the ambiguities are not bad, except for the 2.2-MeV proton case ($\bar{\rho}$ = 82). In addition, τ_1 is plotted as a function of $\bar{\rho}$.

2.1.2. Temperature Dependence

Several sources of data on the temperature dependence of the light output of CsI(0.1% molar Tl) have been published.[9-11] Here the results obtained by Robertson, Lynch, and Jack (RLJ)[9] are used because the techniques and nomenclature employed are essentially the same as SJW which was the basis for the analysis just presented. RLJ present data on the temperature dependence of τ_1, τ_2, ε_∞, R_1, and R_2 for CsI(0.1% molar Tl) excited by 14-MeV protons ($\bar{\rho}$=27.5) and 5.3-MeV alphas ($\bar{\rho}$=396). Their data are reproduced in table 2.

In the present work these data are analyzed in terms of eq. (1) to determine the temperature dependence of a_1 and a_2 in the vicinity of room temperature. In order to simplify the analysis, it is assumed that the temperature dependence and the ionization-density dependence of all parameters in eq. (1) are independent. RLJ obtained the following results for the temperature dependence of the decay time constants:

$$\tau_1(\bar{\rho}=27.5,\ T) \propto e^{917/T},$$

$$\tau_1(\bar{\rho}=396,\ T) \propto e^{1068/T},$$

$$\tau_2(\bar{\rho}=27.5,\ T) \propto e^{720/T},$$

where T is the temperature in degrees Kelvin. No results for τ_2 ($\bar{\rho}$=396, T) are presented. Note that the temperature dependence of τ_1 does have some ionization-density dependence. This small effect is neglected and it is assumed that

$$\tau_1(T) \propto e^{1000/T},$$

independent of $\bar{\rho}$. In addition, it is assumed that

$$\tau_2(T) \propto e^{720/T},$$

independent of $\bar{\rho}$.

With the temperature dependence of the time constants specified, the data from RLJ on ε_∞, R_1, and R_2 (see table 2) are used to solve a_1 and a_2 as functions of temperature since:

$$R_1 = a_i\tau_i/(a_1\tau_1 + a_2\tau_2)$$
$$= a_i\tau_i/\varepsilon_\infty.$$

and therefore,

$$a_i = R_i\varepsilon_\infty/\tau_i.$$

TABLE 2

Exciting Radiation	T (°K)	ε_∞ (a)	R_1	R_2
14-MeV protons	213	1.02	0.39	0.61
	293	1.25	0.55	0.45
	373	0.69	0.93	0.07
5.3-MeV alphas	233	0.519	1.00	0
	273	0.526	0.86	0.14
	293	0.511	0.75	0.25
	353	0.368	1.00	0

(a) Relative values of ε_∞ as a function of T are taken from Figure 6 of RLJ and are normalized to the absolute value at room temperature obtained in Section 2.1.1.

The values of a_1 and a_2 obtained in this way were normalized to the values of room temperature (T=300 K) obtained in Section 2.1.1. and are plotted as a function of temperature in fig. 5. Here a_1 appears to be a linear function of temperature with a coefficient of about one percent per degree. The behavior of a_2 is apparently more complex; it appears to fall both above and below temperatures of 300°K.

2.1.3. Spectral Dependence

Dependence of the spectral response of CsI(Tl) on the ionization density has been reported by Hrehuss,[12] while no dependence was found in a similar study by Gwin and Murray.[13] The existence of two components, with very different time constants (approximately a factor of 10), lead one to hope that they will contribute to different portions of the light emission spectrum, as a function of the stimulating radiation.[11] Measurements such as those reported by Hrehuss and by Gwin and Murray were performed also in the present work using alpha particles from an ^{241}Am source and gamma rays from a ^{57}Co source. No variations, greater than 15% in the integrated intensity, were observed over the spectral range of 380 to 750 nm. This result is consistent with the measurements of Gwin and Murray (reproduced in fig. 6) for 0.17% molar thallium concentration. The reasons for the significant disagreement with the results of Hrehuss are not well understood. Specific activator concentration or the presence of additional impurities are possible explanations.

The way in which the present measurements were performed, essentially an averaging technique summing over many pulses, indicates only that the time-integrated spectrum of light emission does not depend on

ionization density. To determine if the time constants or the relative amplitudes exhibit a spectral dependence, individual pulse shapes were examined using a broad-band response photomultiplier tube (RCA C31000A) and a series of color filters spanning the range of the emission spectrum of CsI(Tl). To within the measurement errors, corresponding to an uncertainty of $\pm 10\%$ in the short time constant τ_1, there is no dependence of the pulse shape on the portion of the spectrum observed for either alpha particle (high ionization density) or cosmic-ray muon (low ionization density) irradiation. This observation is consistent with the measurements reported by Sastry and Thosar.[13]

2.2. Sodium-Activated CsI

2.2.1. Surface Phenomenon

Initial attempts to measure the pulse-shape response of CsI(Na) to irradiation by 4.8-MeV alpha particles yielded anomalous and surprising results. The pulses were an order of magnitude smaller than expected and of only 30-nsec duration, as shown in fig. 7. Because of the very short range of the alpha particles, it was speculated that the observations were related to hydration of the sodium activator at the scintillator surface. To test this hypothesis, the CsI(Na) sample was chipped, and the alpha-particle source was placed on the freshly exposed surface. The pulses observed for the next several hours were characteristic of those expected in CsI(Na), but in four-days time were predominantly of the anomolous variety first observed. In consultation with personnel at Harshaw,[15] it was concluded that the small, fast pulses are the scintillation response of deactivated CsI, the result

of NaOH formation in the scintillator surface. Although similar checks were subsequently performed with samples of CsI(Tl), no such phenomenon was ever observed.

2.2.2. Ionization-Density Dependence

For the pulse-shape response of CsI(Na) Keszthelyi-Landori and Hrehuss[16] report that the relative amplitudes of the two components, but not the decay time constants, depned on ionization density. This leads to very small pulse-shape differences for times less than 4 μsec. Measurements from this work with cosmic-ray muons and 4.8-MeV alpha particles are shown in fig. 8. The observed pulse shapes are consistent with the results of Keszthelyi-Landori and Hrehuss.

Apparently contradictory results of Winyard, Lutkin, and McBeth[17] shows a large pulse-shape difference between 4.8-MeV alpha particles and gamma rays in CsI(Na). Such a large difference could be due to the anomolous surface behavior of CsI(Na) discussed previously.

Since the scintillation response of CsI(Na) exhibited less promise for pulse-shape discrimination than the response of CsI(Tl), subsequent efforts to use CsI as a particle discriminator were limited to thallium-activated material.

3. PULSE SHAPE DISCRIMINATION

The response of CsI(Tl) was investigated to determine if the time-dependent pulse shape would adequately distinguish between interacting hadrons and electron-induced electromagnetic cascades with comparable total energy deposition.

3.1. BNL Measurements

Measurements of the pulse-shape response of CsI(Tl) to 14 GeV/c negative pions were performed at Brookhaven National Laboratory in August, 1972. Interacting pions were distinguished by pulse height. In fig. 9, the time dependence of the response of CsI(Tl) to a non-interacting and to an interacting pion are shown. The pulse height corresponding to the interacting pion is approximately 50 times that of the noninteracting pion. The short time constants, τ_1 were determined for these pulses in the same manner as the τ_1 for the pulses in fig. 1. For the noninteracting pion, $\tau_1 = 0.78 \pm 0.08$ μsec, the same as for cosmic ray muons. For the interacting pion, $\tau_1 = 0.71 \pm 0.08$ μsec, less by about 10%, but the difference lies within the experimental resolution of the measurements.

3.2. SLAC Measurements

Preliminary tests to evaluate the feasibility of distinguishing between electrons and interacting pions by pulse shape discrimination in CsI(Tl) were performed as part of an experiment at the Stanford Linear Accelerator Center in April, 1972. The complete apparatus is described previously.[18] Of particular interest here is the front portion of the ionization spectrometer which consisted of several 2-cm thick CsI(Tl)* crystals. Each crystal is approximately one radiation lengths thick. The assembly was exposed to electrons and pions at 5, 10, and 15 GeV/c. The scintillators were viewed by RCA 4523 or 4463 photo-multiplier tubes (PMT) through acrylic lightguides. These PMT are identical except for the spectral response of the photocathodes. The 4523 has a

*Purchased from Quartz et Silice, S. A., Paris, France.

bialkali photocathode and the 4463 has an S-20 photocathode that has more sensitivity towards the red end of the visible spectrum. The current pulses from the PMT were simultaneously pulse-height and pulse-shape analyzed. The pulse shape analysis was conventional and consisted of measurement of the time to zero-crossing of the CsI pulses after a single RC-integration followed by double RC-differentiation. The measured distributions for 15-GeV/c electrons and interacting*, 15-GeV/c pions in the first three CsI crystals are presented in fig. 10-a, -b, and -c. The histograms are one-dimensional projections that were obtained by integration of the two-dimensional distributions (in pulse-height and pulse-shape) over all pulse heights greater than 2.7 times single minimum ionizing. Examination of the two-dimensional distributions showed that the measured pulse shape parameter (time to zero-cross) is independent of pulse height over the range of integration. For all three crystals the pulse heights observed for interacting pions ranged up to about 50 times minimum ionizaing. For electrons, they extended up to about 15, 50, and 100 times minimum ionizing for crystals 1, 2, and 3, respectively.

It is evident from the observed results that there is a small but consistent difference between the electron and pion distributions. In all three cyrstals the mean values of the time to zero-crossing for electrons is about 30 nsec longer than that for pions. For the circuits used in these measurements this difference corresponds to an effective, single decay-time constant that is 10 percent longer for electrons than

*The counter in which the pion apparently first interacts is determined by analysis of the measured pulse heights in the CsI and the following tungsten modules.

for interacting pions. Thus, we have a pulse shape difference that is consistent with the BNL observations and that is at best marginally useful for electron-hadron discrimination. A conclusive effort would necessarily involve an investigation of interacting protons in CsI, as well as interacting pions, which were employed for convenience in the present work.

ACKNOWLEDGEMENTS

The authors wish to thank Drs. J. F. Arens, C. Orth and S. Verma for informative and stimulating discussions. The authors also wish to thank Prof. H. Crannell, Dr. A. J. Fisher, and Mr. G. Vaughn-Cooke for assistance with the BNL portion of these measurements and Dr. C. Orth for assistance with the SLAC portion. The interest and support of Dr. J. F. Ormes and Prof. H. Whiteside in this work are sincerely appreciated.

REFERENCES

1) T. M. K. Marar, P. S. Freier, and C. J. Waddington, J. Geophys. Res. 76 (1971) 1625.

2) W. R. Webber and J. M. Rockstroh, J. Geophys. Res. 78 (1973) 1.

3) P. Meyer, Invited Papers and Rapporteur Talks, Twelfth Int. Conf. on Cosmic Rays, Tasmania (1971).

4) R. F. Silverberg, J. F. Ormes, and V. K. Balasubrahmanyan (to be published in J. Geophys. Res.).

5) A. Buffington, G. F. Smoot, L. H. Smith, and C. A. Orth, SSL Ser 14, Issue 35 (1973) 126-1; and Paper 126, Thirteenth International Cosmic Ray Conference, Denver (1973).

6) C. J. Crannell, W. V. Jones, R. J. Kurz, R. F. Silverberg, and W. Viehmann, Paper 341, Thirteenth International Cosmic Ray Conference, Denver (1973).

7) R. S. Storey, W. Jack, and A. Ward, Proc. Phys. Soc. 72 (1958) 1.

8) M. J. Berger and S. M. Seltzer, NASA Report SP-3012 (1964).

9) W. H. Barkas and M. J. Berger, NASA Report SP-3013 (1964).

J. R. Janni, Air Force Weapons Laboratory Report AFWL-TR-65-150 (1966).

J. C. Robertson, J. G. Lynch, and W. Jack, Proc. Phys. Soc. 78 (1961) 1188.

10) F. E. Senftle, P. Martinez, and B. P. Alekna, Rev. Sci. Instr. 33 (1962) 819.

11) W. W. Managan, IRE Trans. Nucl. Sci. NS-9 (1962) 1.

12) R. Gwin and R. B. Murray, Oak Ridge National Laboratory Report ORNL 3354 (1962);

Phys. Rev. 131 (1963) 501; and

Phys Rev. 131 (1963) 508.

13) G. Hrehuss, Nucl. Instr. and Methods 8 (1960) 344.

14) N. P. Sastry and B. V. Thosar, Proc. Ind. Acad. Sci. 54 A (1961) 140.

15) M. R. Farukhi, Harshaw Chemical Corporation, private communication.

16) S. Keszthelyi-Landori and G. Hrehuss, Nucl Instr. and Methods 68 (1969) 9.

17) R. A. Winyard, J. E. Lutkin, and G. W. McBeth, Nucl Instr. and Methods 95 (1971) 141.

18) D. L. Cheshire, R. W. Huggett, W. V. Jones, S. P. Rountree, S. D. Verma, W. K. H. Schmidt, R. J. Kurz, T. Bowen, E. P. Kreider, Paper 133, Thirteenth International Cosmic Ray Conference, Denver, (1973).

APPENDIX A. CsI PROPERTIES

Bibliography

D. W. Aitken, B. L. Beron, G. Yenicay, and H. R. Zulliger
Stanford University, High Energy Physics Laboratory
Report HEPL-478; and IEEE Trans. Nucl. Sci. NS-14 (1967) 468.

J. B. Birks, IEEE Trans. Nucl. Sci. NS-9 (1962) 4.

J. W. Blue and D. C. Liu, IRE Trans. Nucl. Sci. NS-9 (1962) 48.

R. Gwin and R. B. Murray, Oak Ridge National Laboratory Report ORNL-3354 (1962); Phys Rev. 131 (1963) 501; and Phys. Rev. 131 (1963) 508.

G. Hrehuss, Nucl. Instr. and Methods 8 (1960) 344.

S. Keszthelyi-Landori and G. Hrehuss, Nucl. Instr. and Methods 68 (1969) 9.

H. Knopfel, E. Loepfe, and P. Stoll, Helv. Phys. Acta, 30 (1957) 521.

W. W. Managan, IRE Trans. Nucl. Sci. NS-9 (1962) 1.

J. C. Robertson and J. G. Lynch, Proc. Phys. Soc. 77 (1961) 751.

J. C. Robertson, J. G. Lynch, and W. Jack, Proc. Phys. Soc. 78 (1961) 1188.

N. P. Sastry and B. V. Thosar, Proc. Inc. Acad. Sci. 54 A (1961) 140.

F. E. Senftle, P. Martinez, and B. P. Alekna, Rev. Sci. Instr. 33 (1962) 819.

R. S. Storey, W. Jack, and A. Ward, Proc. Phys. Soc. 72 (1958) 1.

J. L. Tidd, J. R. Dabbs, and N. Levine, Marshall Space Flight Center Report NASA TM-X-64741 (1973).

E. A. Womack, A. J. Lazarus, and M. Joseph, IEEE Trans. Nucl. Sci. NS-11 (1964) 24.

APPENDIX B. PULSE SHAPE DISCRIMINATION TECHNIQUES

Bibliography

T. K. Alexander and F. S. Goulding, Nucl. Instr. and Methods 13 (1961) 244.

R. Bass, W. Kessel, and G. Majoni, Nucl. Instr. and Methods 30 (1964) 237.

J. P. Crettez, S. Cambou, and G. Ambrosino, Nuclear Electronics Proceedings of the Belgrade Conference 2 (1961) 287.

M. F. D'Cunha and G. Joseph, Nucl. Instr. and Methods 95 (1971) 515.

M. Forte, A. Konsta, and C. Maranzana, Nuclear Electronics Proceedings of the Belgrade Conference 2 (1961) 277.

R. Fulle, Gy. Mathe, and D. Metzband, Nucl. Instr. and Methods 35 (1965) 250.

E. Gatti and F. De Martini, Nuclear Electronics Proceedings of the Belgrade Conference 2 (1961) 265.

L. J. Heistek and L. Van der Zwan, Nucl. Instr. and Methods 80 (1970) 213.

A. Joblin, Ph.D. Thesis, Drexel Institute of Technology (1969); University Microfilms 69-18247.

Gy. Mathe, Nucl. Instr. and Methods 39 (1966) 356.

Gy. Mathe and B. Schlenk, Nucl. Instr. and Methods 27 (1964) 10.

G. W. McBeth, J. E. Lutkin, and R. A. Winyard, Nucl. Instr. and Methods 93 (1971) 99.

E. Nadav and B. Kaufman, Nucl. Instr. and Methods 33 (1965) 289.

R. B. Owen, IRE Trans. Nucl. Sci. NS-9 (1962) 285.

J. C. Robertson and A. Ward, Proc. Phys. Soc. 73 (1959) 523.

M. L. Roush, M. A. Wilson, and W. S. Hornyak, Nucl. Instr. and Methods 31 (1964) 112.

W. Schweimer, Nucl. Instr. and Methods 39 (1966) 343.

Y. Takami and M. Hosoe, Nucl. Instr. and Methods 31 (1964) 347.

L. Varga, Nucl. Instr. and Methods 14 (1961) 24.

R. A. Winyard, J. E. Lutkin, and G. W. McBeth, Nucl. Instr. and Methods 95 (1971) 141.

FIGURE CAPTIONS

Figure 1. Time-dependent response of CsI(Tl), viewed by an RCA C31000A photomultiplier tube, to 5.3-MeV alpha-particle and cosmic-ray muon radiation.

Figure 2. Integrated time-dependent response of CsI(Tl), viewed by an RCA 8575 photomultiplier tube, to 4.8-MeV alpha-particle and cosmic-ray muon radiation. The points are from the data presented in Reference 7.

Figure 3-a, -b, -c, -d. Plots of the relationships between the amplitudes a_1 and a_2 from the data in Reference 7 for 0.662-MeV photons, 8.6-MeV protons, 2.2-MeV protons, and 4.8-MeV alpha particles, respectively.

Figure 4. The values of a_1, a_2, and τ_1 obtained from fig. 3 as a function of $\overline{\rho}$.

Figure 5. The relative values of a_1 and a_2, obtained from the data in Reference 9, as a function of temperature.

Figure 6. The spectral response of CsI(Tl) reproduced from ORNL 3354, Reference 12.

Figure 7. Anomalous time-dependent response of CsI(Na), viewed by an RCA 8575 photomultiplier tube, to 4.8-MeV alpha particles.

Figure 8. Time-dependent response of CsI(Na), used in conjunction with an RCA 8575 photomultiplier tube, to 4.8-MeV alpha particle and cosmic-ray muon irradiation.

Figure 9. Time-dependent response of CsI(Tl), used in conjunction with an RCA 8575 photomultiplier tube, to interacting and non-interacting 14-GeV negative pions.

Figure 10-a, -b, -c. Time-dependent distributions of the response of CsI(Tl) to electron-induced electromagnetic cascades and interacting pions. The detector samples were arranged in consecutive one-radiation-length-thick layers.

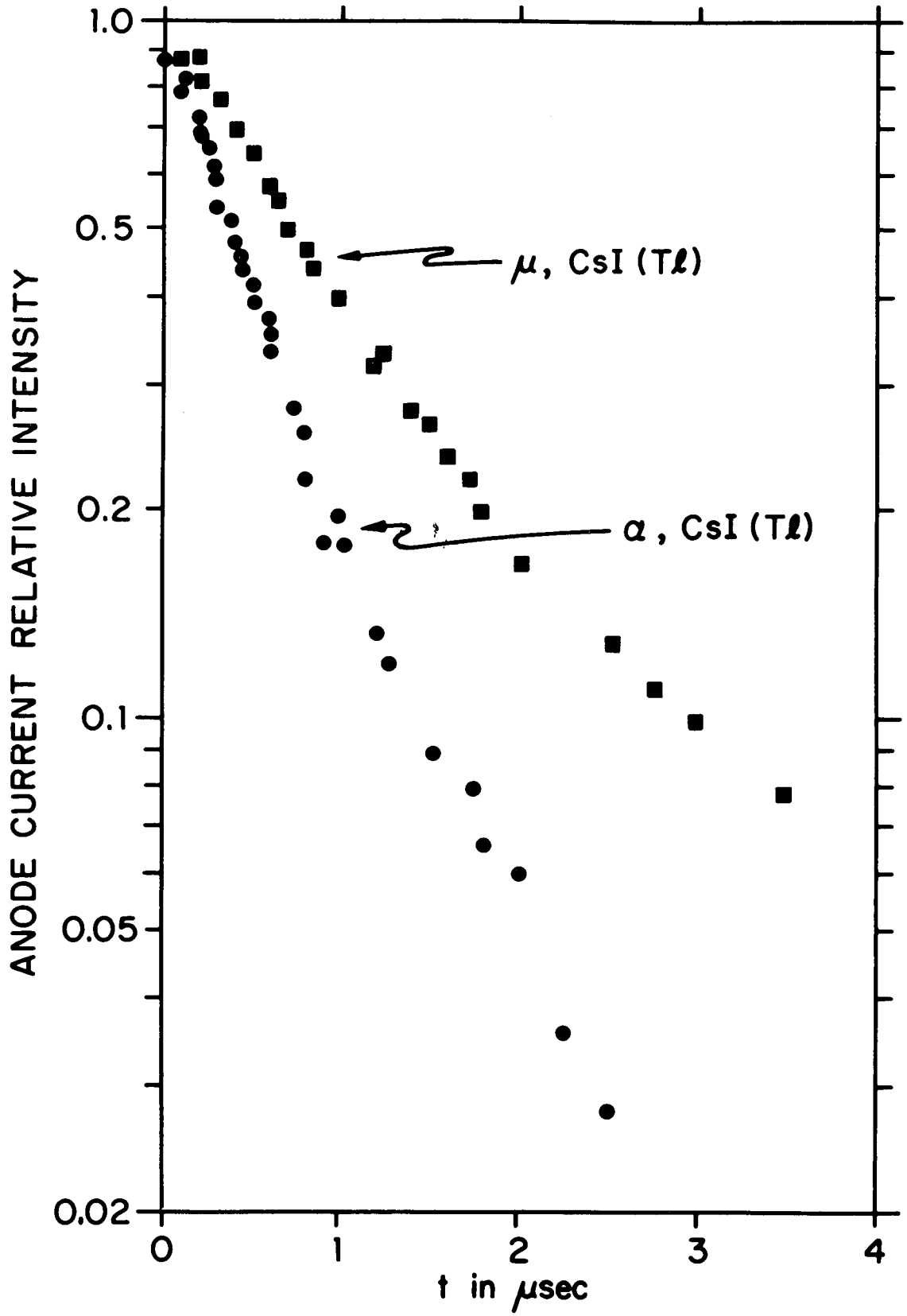
1.0
0.5
0.2
0.1
0.05
0.02
ANODE CURRENT RELATIVE INTENSITY
μ, CsI (Tℓ)
α, CsI (Tℓ)
0
1
2
3
4
t in μsec

Figure 1

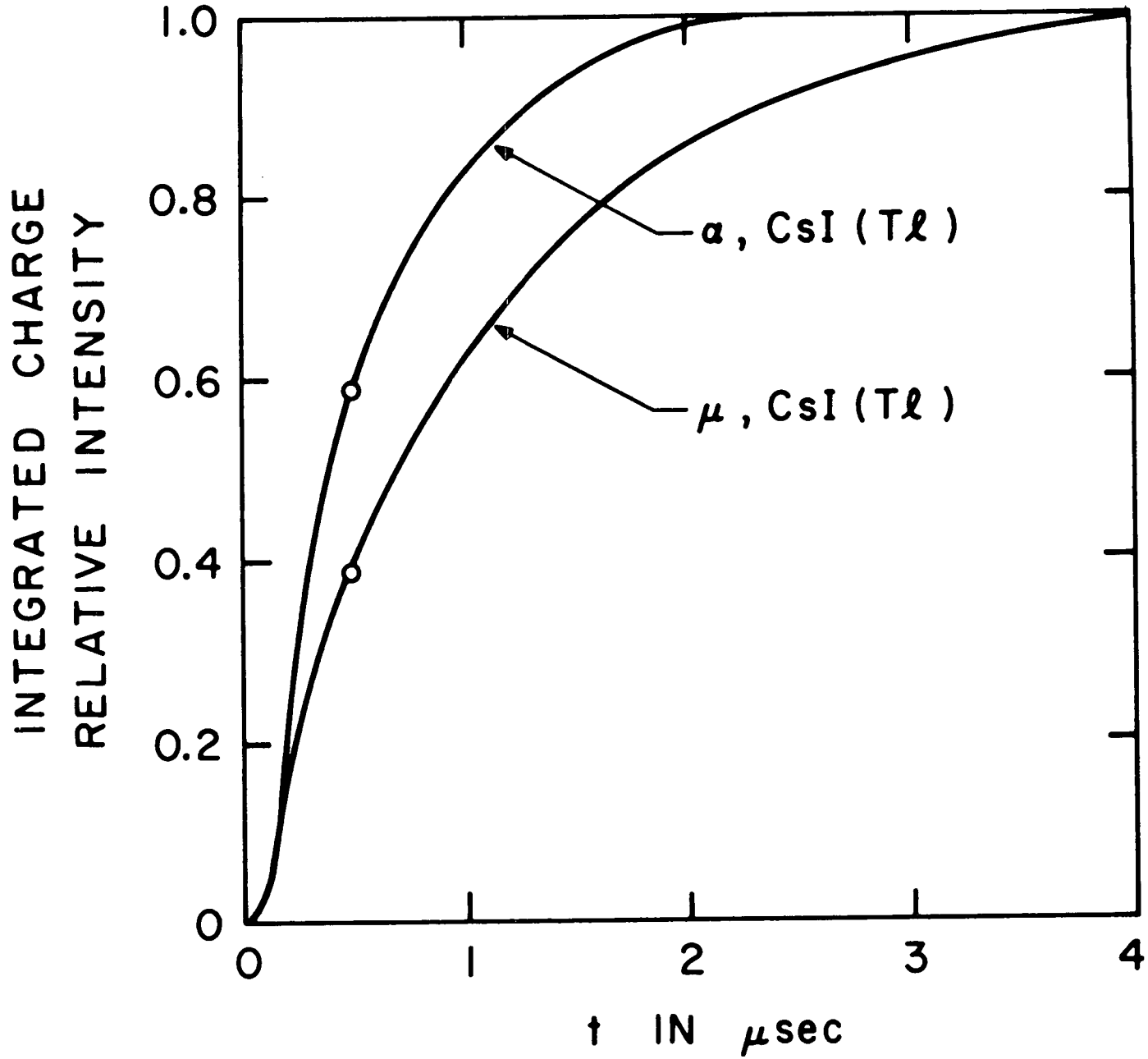
INTEGRATED CHARGE
RELATIVE INTENSITY
1.0
0.8
0.6
0.4
0.2
0
0
1
2
3
4
t IN μsec
α, CsI (Tℓ)
μ, CsI (Tℓ)

Figure 2

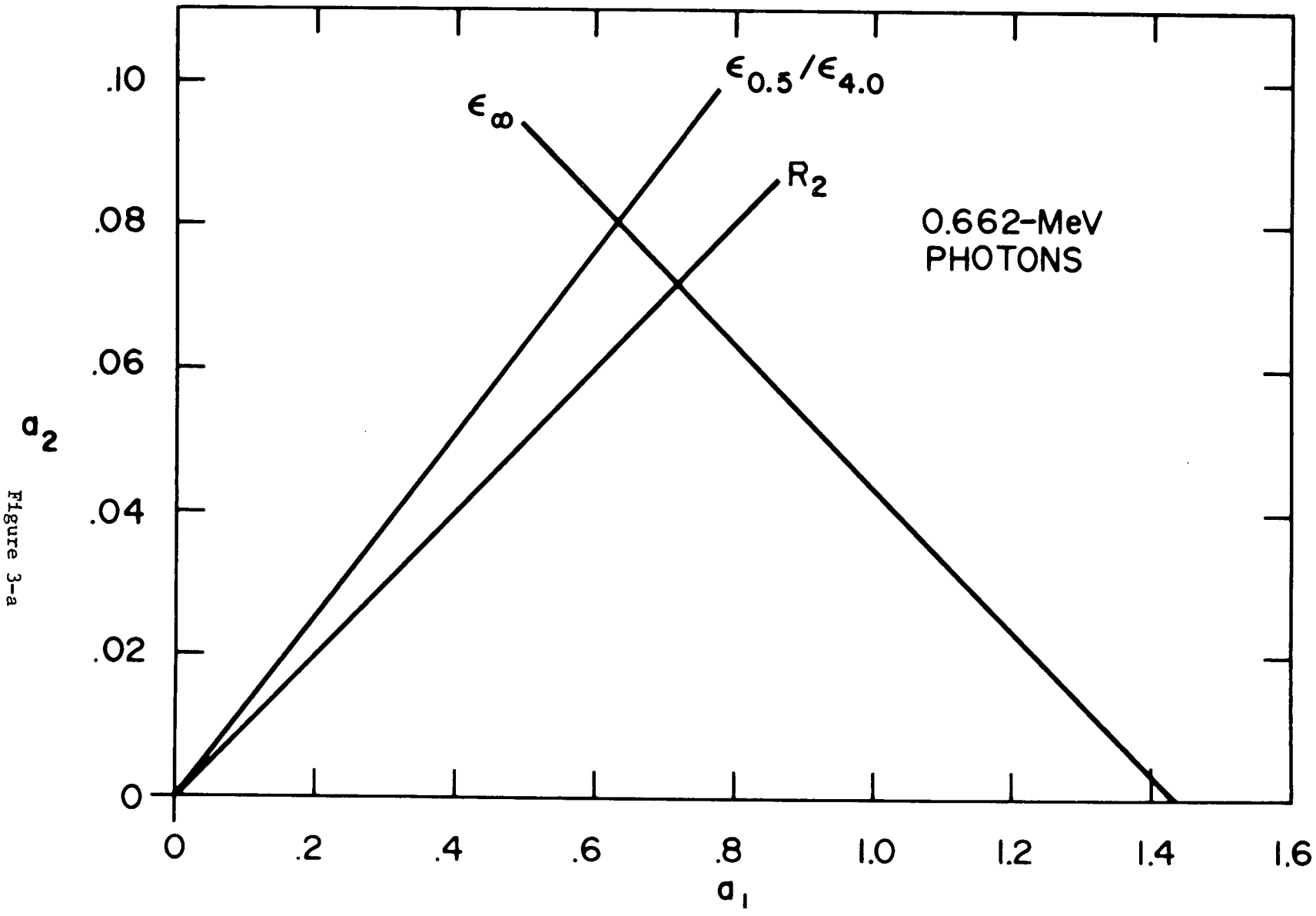
.10
.08
.06
.04
.02
0
a_2
$\epsilon_{0.5}/\epsilon_{4.0}$
ϵ_∞
R_2
0.662-MeV
PHOTONS
0
.2
.4
.6
.8
1.0
1.2
1.4
1.6
a_1

Figure 3-a

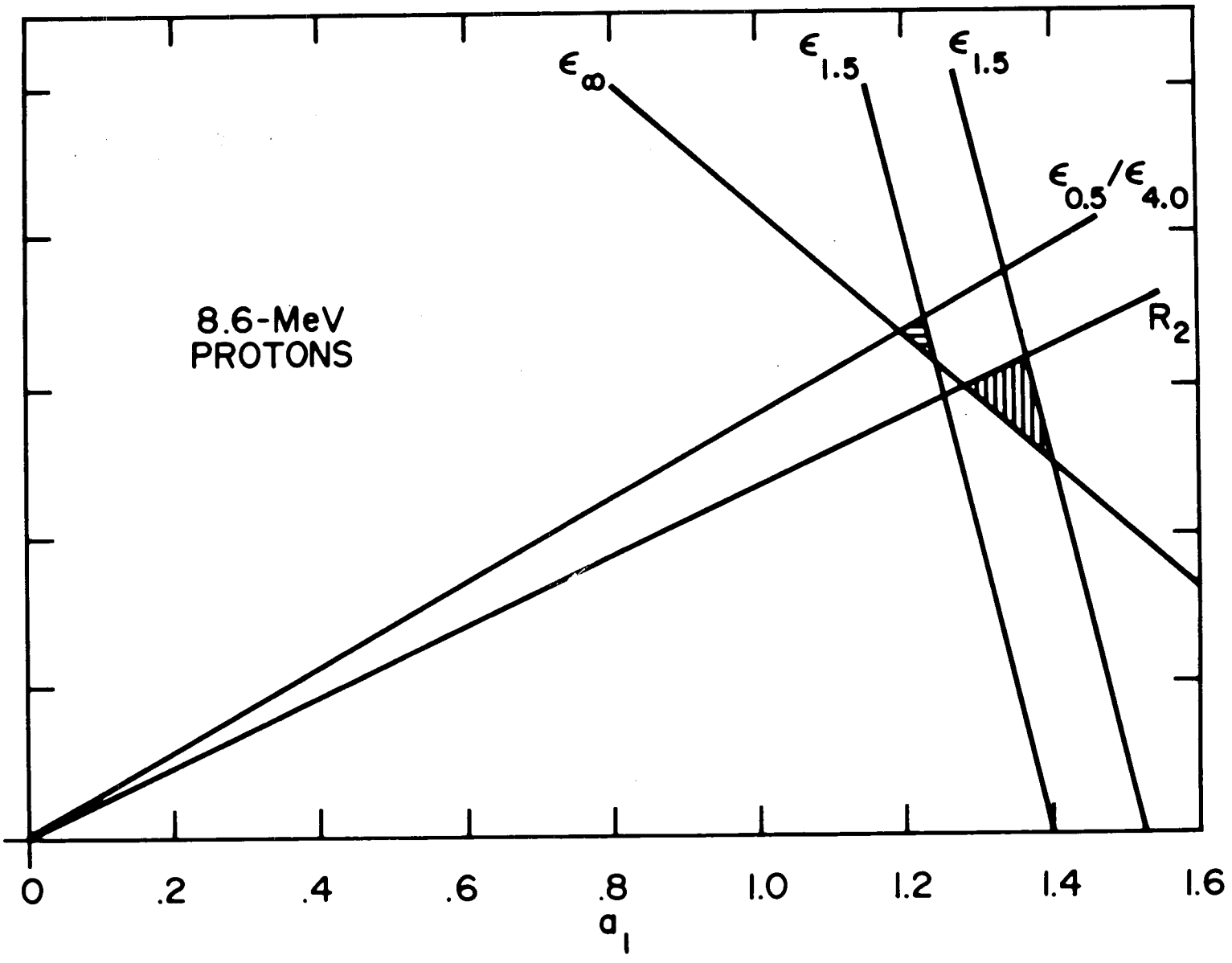
8.6-MeV
PROTONS
ϵ_∞
$\epsilon_{1.5}$
$\epsilon_{1.5}$
$\epsilon_{0.5}/\epsilon_{4.0}$
R_2
a_2
a_1
0
.02
.04
.06
.08
.10
0
.2
.4
.6
.8
1.0
1.2
1.4
1.6

Figure 3-b

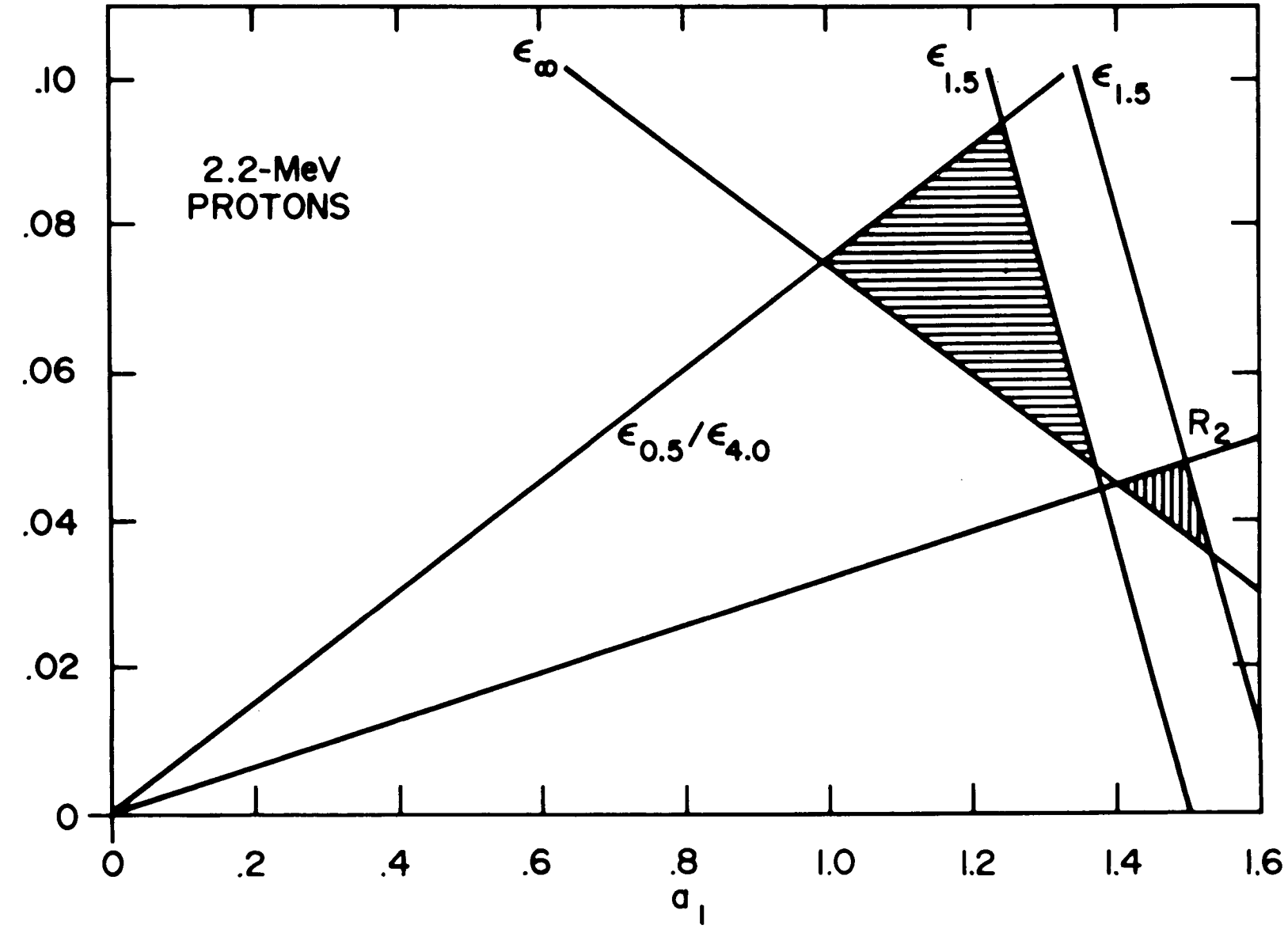
2.2-MeV
PROTONS
ϵ_∞
$\epsilon_{1.5}$
$\epsilon_{1.5}$
$\epsilon_{0.5}/\epsilon_{4.0}$
R_2
a_2
a_1
.10
.08
.06
.04
.02
0
0
.2
.4
.6
.8
1.0
1.2
1.4
1.6

Figure 3-c

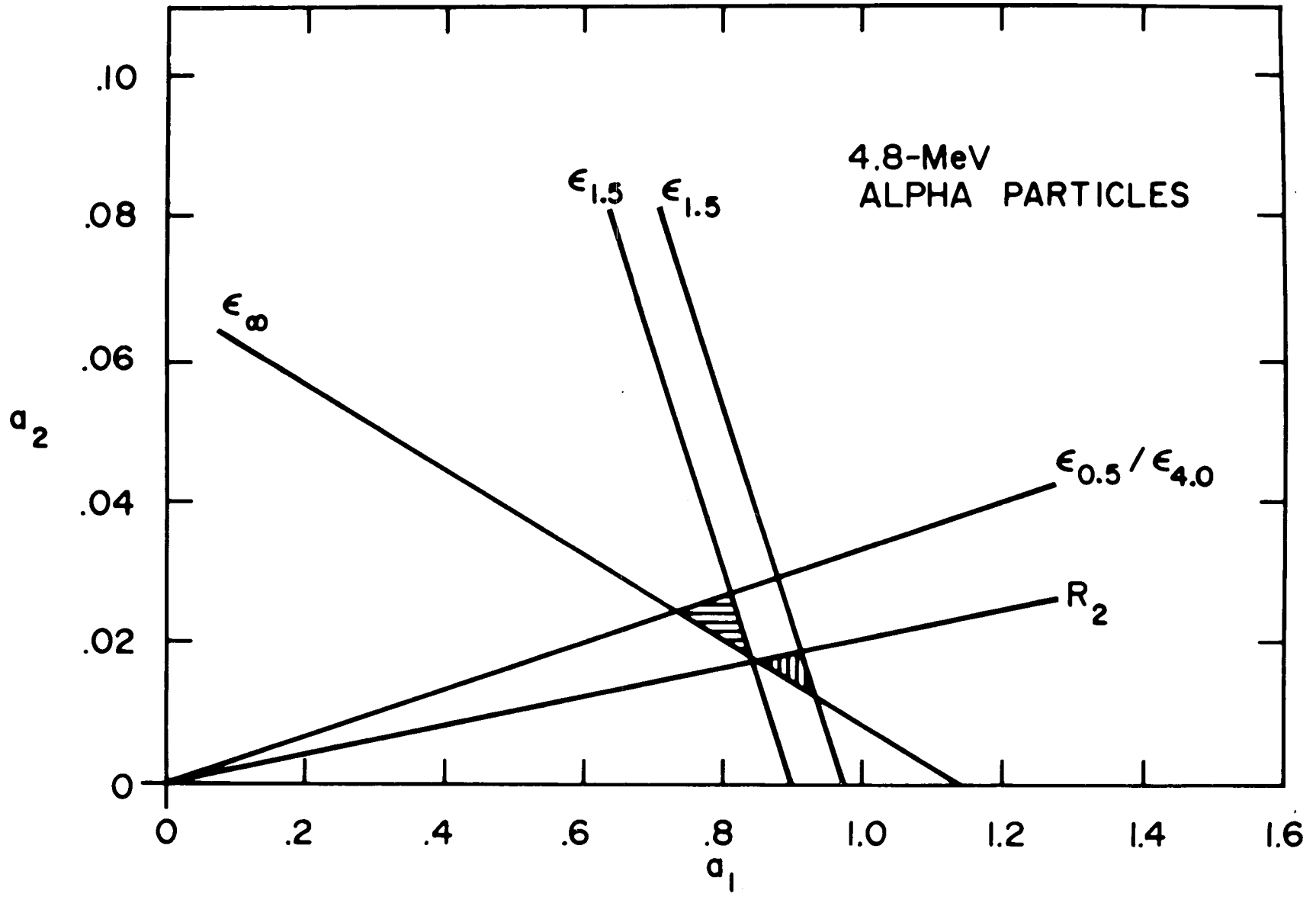
4.8-MeV
ALPHA PARTICLES
$\epsilon_{1.5}$
$\epsilon_{1.5}$
ϵ_{∞}
$\epsilon_{0.5}/\epsilon_{4.0}$
R_2
a_2
a_1
.10
.08
.06
.04
.02
0
0
.2
.4
.6
.8
1.0
1.2
1.4
1.6

Figure 3-d

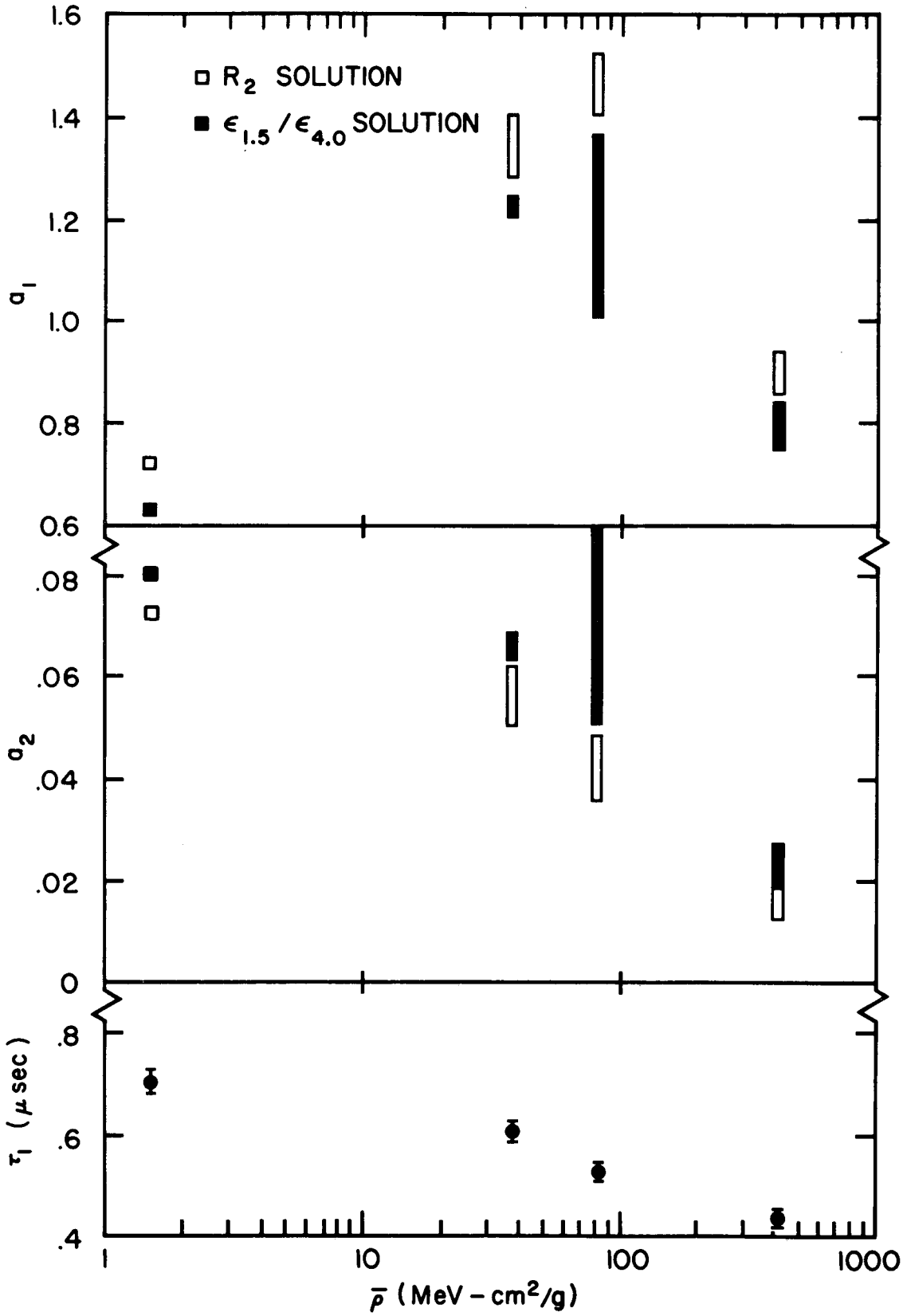
1.6
1.4
1.2
1.0
0.8
0.6
a_1
R_2 SOLUTION
$\epsilon_{1.5}/\epsilon_{4.0}$ SOLUTION
.08
.06
.04
.02
0
a_2
.8
.6
.4
τ_1 (μsec)
1
10
100
1000
$\bar{\rho}$ (MeV - cm^2/g)

Figure 4

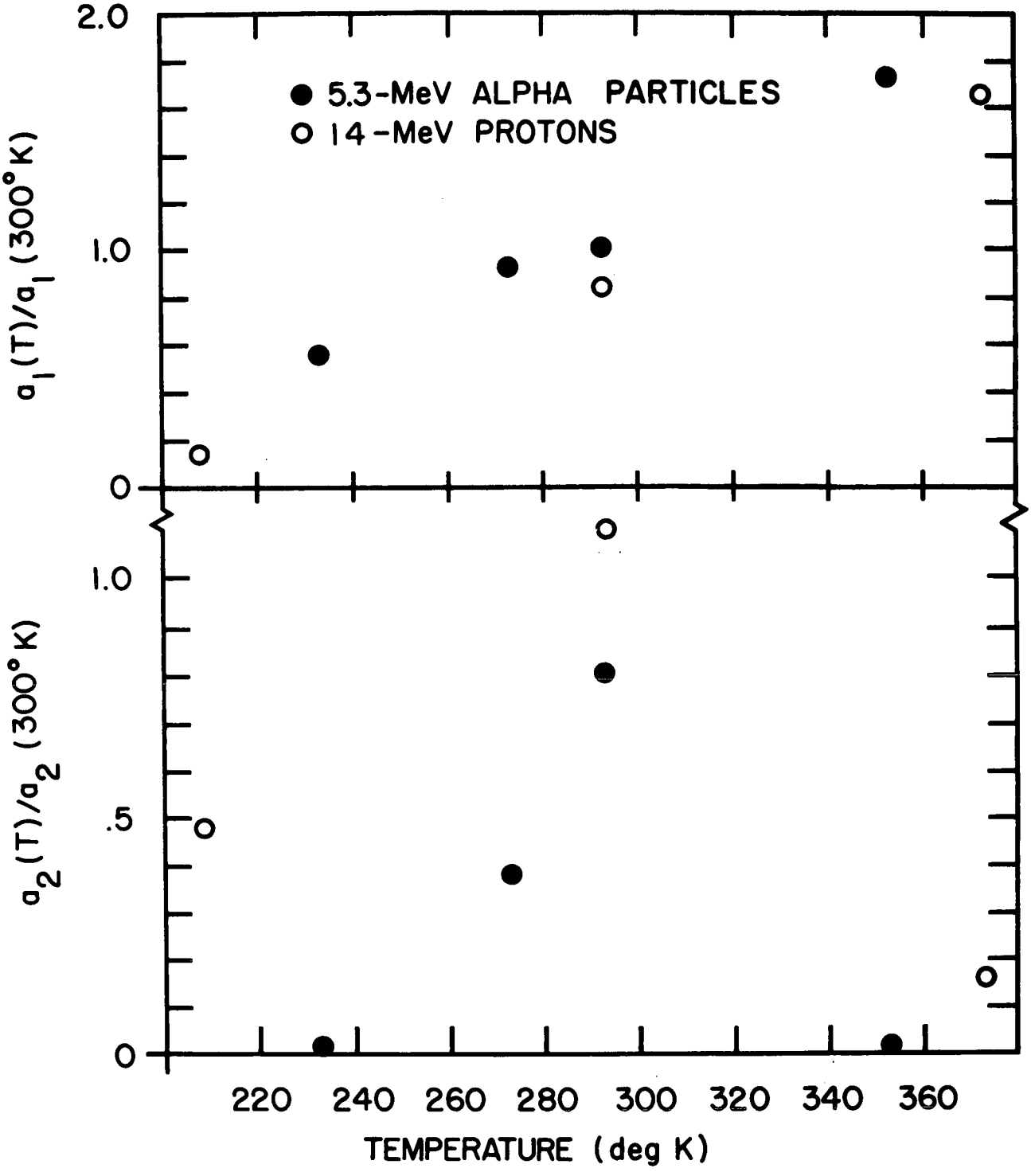
2.0
1.0
0
● 5.3-MeV ALPHA PARTICLES
○ 14-MeV PROTONS
$a_1(T)/a_1(300°K)$
1.0
.5
0
$a_2(T)/a_2(300°K)$
220
240
260
280
300
320
340
360
TEMPERATURE (deg K)

Figure 5

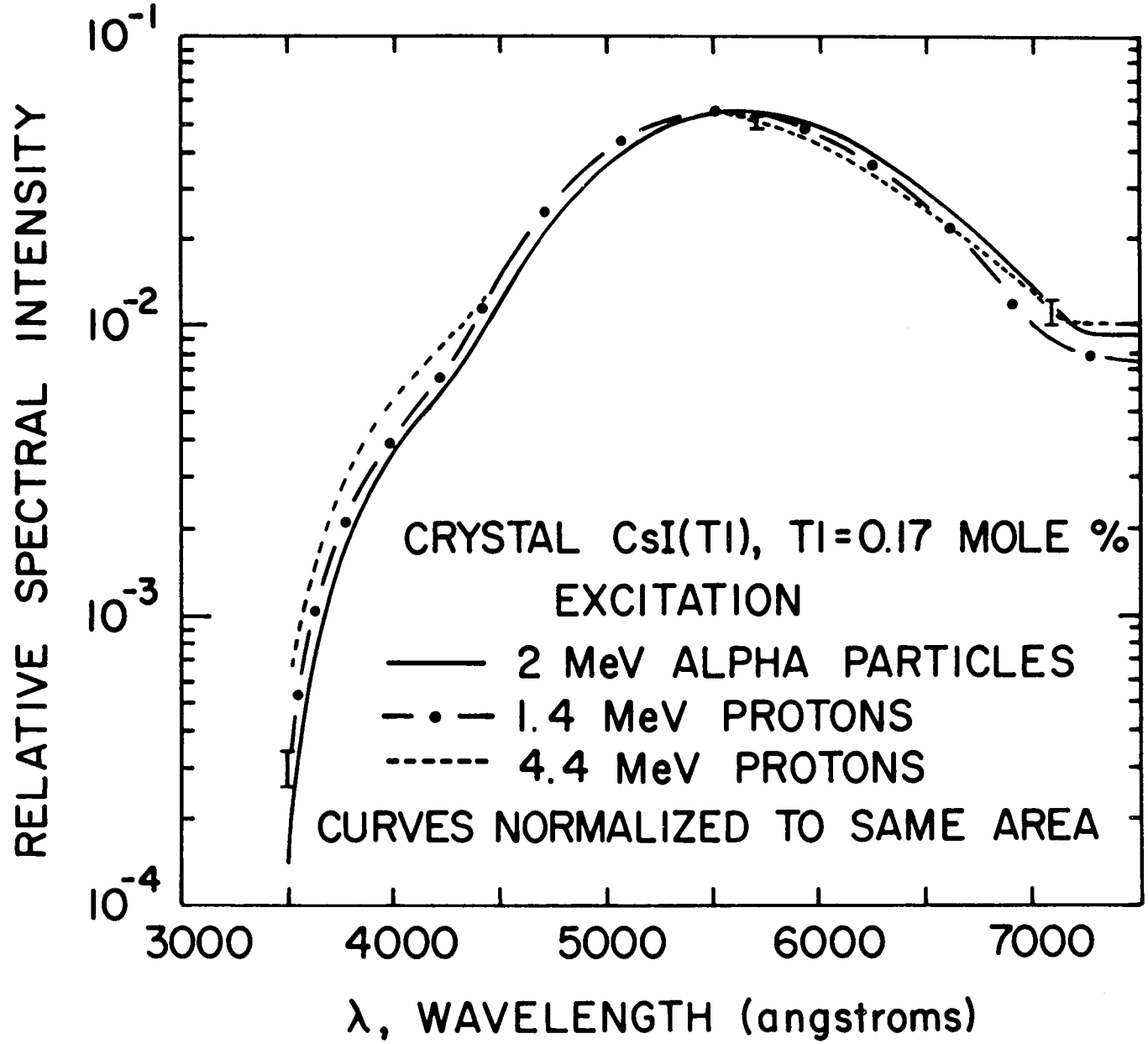
RELATIVE SPECTRAL INTENSITY
10^{-1}
10^{-2}
10^{-3}
10^{-4}
3000
4000
5000
6000
7000
λ, WAVELENGTH (angstroms)
CRYSTAL CsI(Tl), Tl=0.17 MOLE %
EXCITATION
2 MeV ALPHA PARTICLES
1.4 MeV PROTONS
4.4 MeV PROTONS
CURVES NORMALIZED TO SAME AREA

Figure 6

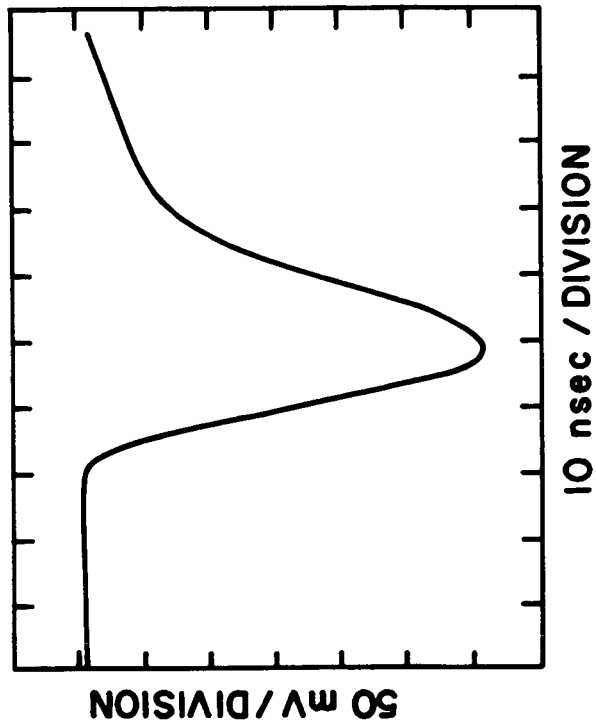

Figure 7

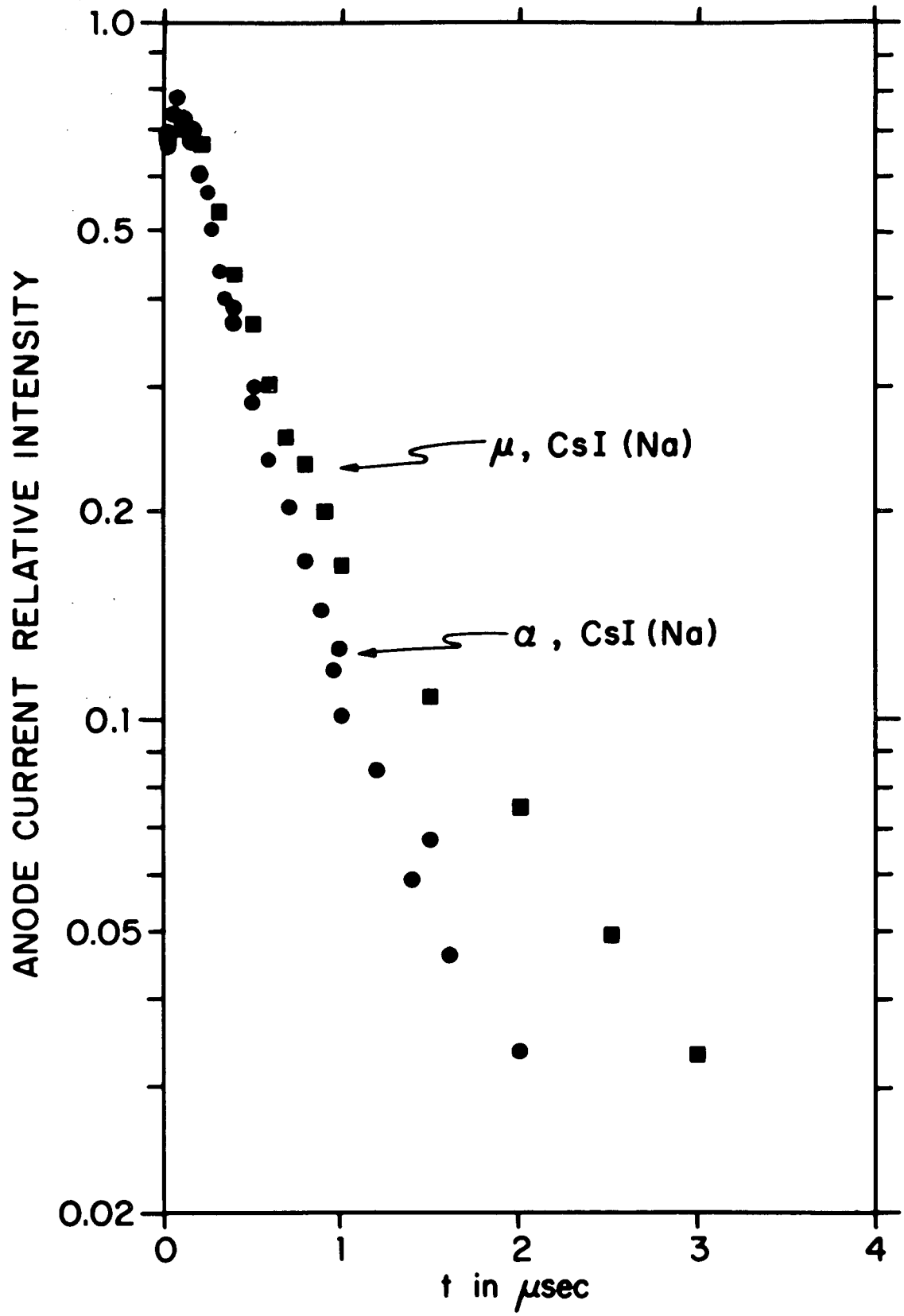
1.0
0.5
0.2
0.1
0.05
0.02
ANODE CURRENT RELATIVE INTENSITY
μ, CsI (Na)
α, CsI (Na)
0
1
2
3
4
t in μsec

Figure 8

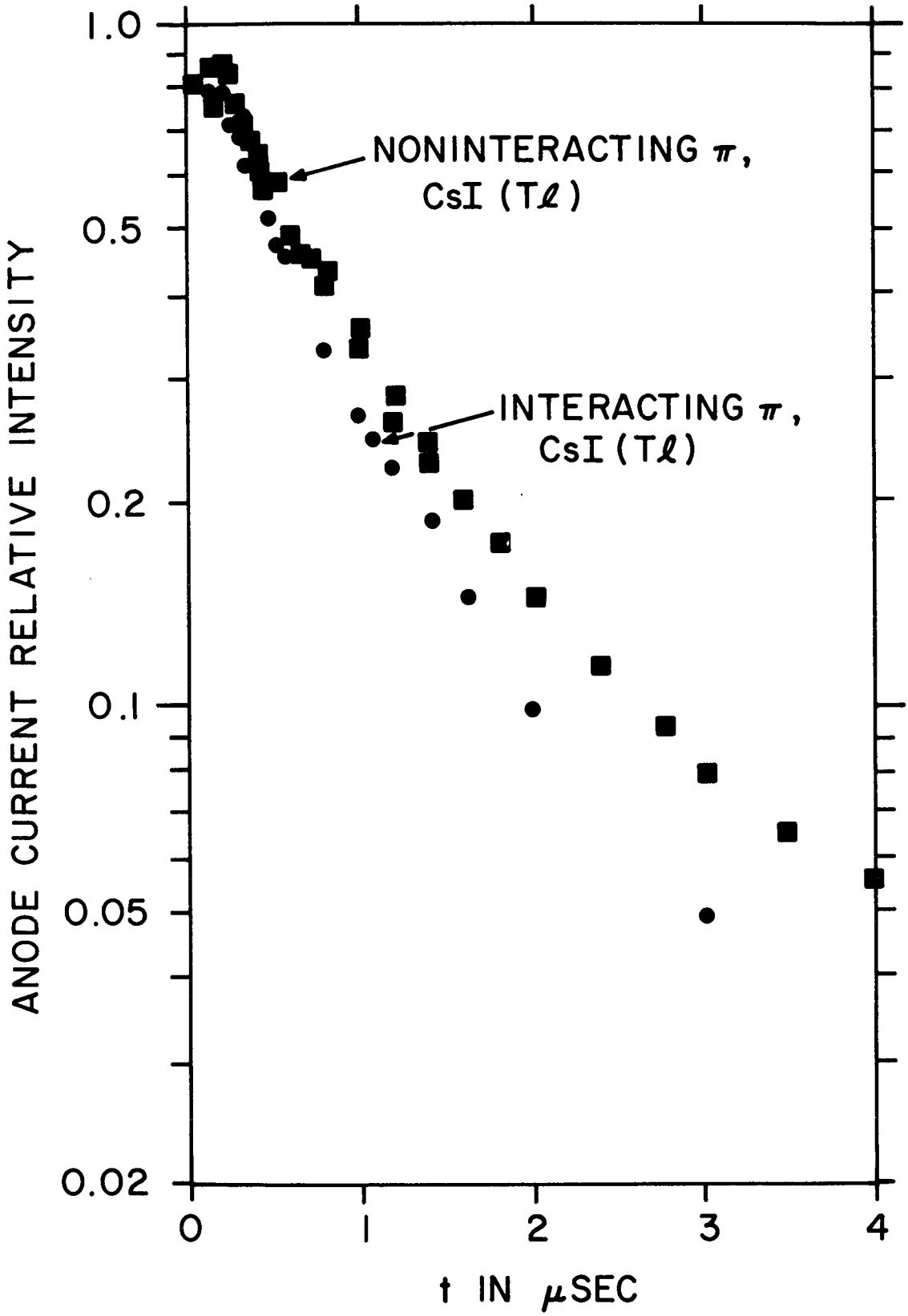
1.0
0.5
0.2
0.1
0.05
0.02
ANODE CURRENT RELATIVE INTENSITY
NONINTERACTING π,
CsI (Tℓ)
INTERACTING π,
CsI (Tℓ)
0
1
2
3
4
t IN μSEC

Figure 9

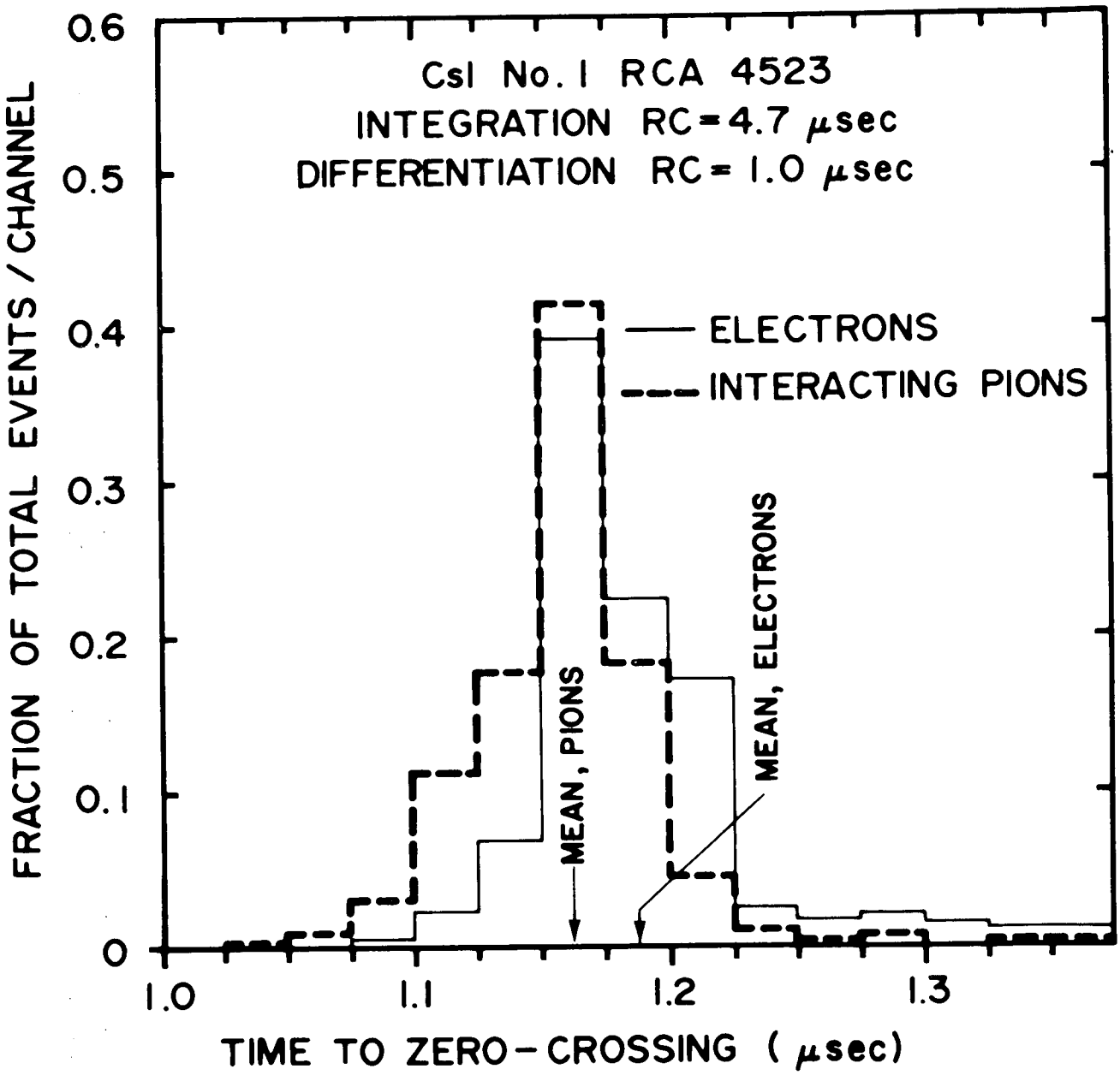
CsI No. 1 RCA 4523
INTEGRATION RC = 4.7 μsec
DIFFERENTIATION RC = 1.0 μsec
ELECTRONS
INTERACTING PIONS
MEAN, PIONS
MEAN, ELECTRONS
FRACTION OF TOTAL EVENTS / CHANNEL
TIME TO ZERO-CROSSING (μsec)
0.6
0.5
0.4
0.3
0.2
0.1
0
1.0
1.1
1.2
1.3

Figure 10-a

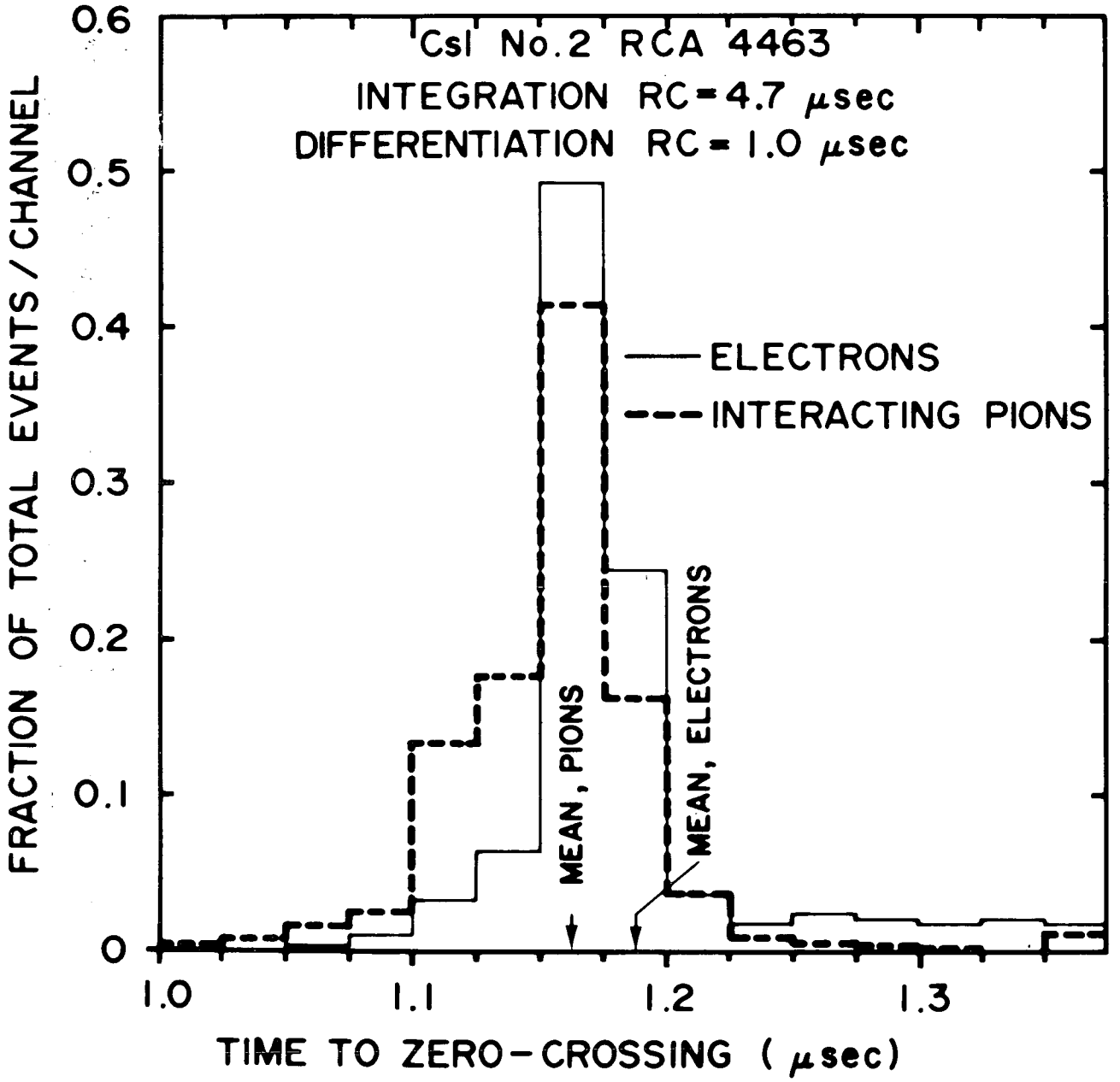
CsI No.2 RCA 4463
INTEGRATION RC = 4.7 μsec
DIFFERENTIATION RC = 1.0 μsec
ELECTRONS
INTERACTING PIONS
MEAN, PIONS
MEAN, ELECTRONS
FRACTION OF TOTAL EVENTS / CHANNEL
TIME TO ZERO-CROSSING (μsec)
0.6
0.5
0.4
0.3
0.2
0.1
0
1.0
1.1
1.2
1.3

Figure 10-b

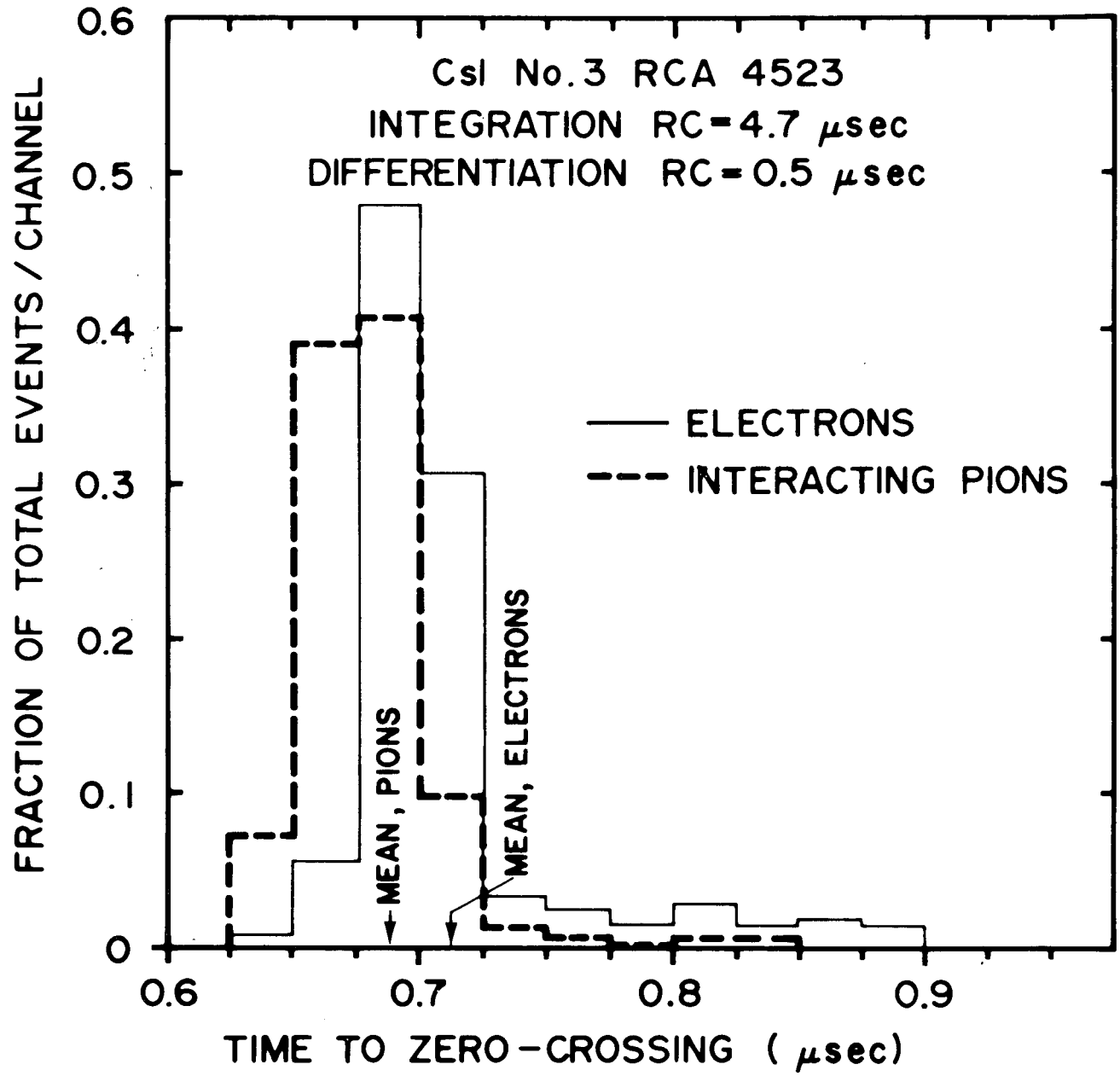

Figure 10-c

NASA–GSFC